East European Journal of Physics. 3. 365-374 (2025)
DOI:10.26565/2312-4334-2025-3-37 ISSN 2312-4334

MAGNETIC AND THERMOELECTRIC PROPERTIES OF RbCaYF(Y = C and N) HEUSLER ALLOYS: PROMISING CANDIDATES FOR EMBEDDED SYSTEMS IN TELECOMMUNICATIONS

Kheira Bahnes[a,b], Saliha Rezini[b], Amel Abbad[a,b], Wissam Benstaali[a,b]*, Noureddine Saidi[a,b], Omar Belarbi[a,b]

[a]*Laboratory of Technology and Solids Properties, Faculty of Sciences and Technology, Abdelhamid Ibn Badis University, Mostaganem, Algeria*
[b]*Faculty of Sciences and Technology, BP227, Abdelhamid Ibn Badis University, Mostaganem (27000), Algeria*
**Corresponding Author E-mail: ben_wissam@yahoo.fr*
Received March 30, 2025; revised July 31, 2025; accepted August 10, 2025

On the basis of density functional theory, the structural, electronic, magnetic and thermoelectric properties of the d0 new quaternary Heusler alloys RbCaYF (Y= C and N) have been analyzed by means of first-principles calculations. The results predict a stable atomic arrangement in Y-type (III) phase with a ferromagnetic order. The two compounds were found to be half-metallic ferromagnets (HMFs) with an integer magnetic moment of 2μB for RbCaCF and 1μB for RbCaNF. The ferromagnetism observed is originated from the polarization of the p-Y orbitals with an sp-hybridization. In addition, RbCaCF and RbCaNF display large half metallic (HM) gaps of 0.879, 0.672 eV using Generalized Gradient Approximation (GGA), and 1.730, 1.934 eV with Generalized Gradient Approximation Modified Becke and Johnson (GGA-mBJ) respectively demonstrating stable half metallic features. Besides, thermoelectric properties were computed over a wide range of temperatures. The two Heusler alloys exhibit high values of electric conductivity and figure of merit especially at high temperatures. RbCaCF and RbCaNF d0 Heusler alloys present high spin polarization, robust half-metallicity and high thermoelectric coefficients, which makes them good candidates for spintronic and thermoelectric applications leading to promising enhancements for embedded systems in telecommunications.
Keywords: *Half-metallic; d0 Heusler Alloys; Embedded systems; Thermoelectric Properties; Telecommunications; Wien2k*
PACS: 71.20.Be; 75.50.Cc; 07.07.Df; 73.50.Lw; 42.79.Sz; 71.20.-b

1. INTRODUCTION

Human activities such as automotive exhaust and industrial processes, along with the emission of CO_2, contribute significantly to adverse climate changes. Thermoelectric (TE) materials are crucial in global efforts toward sustainable energy solutions. They are being studied not only for their ability to convert waste thermal energy directly into useful electrical energy but also for their potential to efficiently mitigate environmental pollution.

In recent years, Heusler alloys have emerged as key materials in spintronic devices [1] due to their high Curie temperature and 100% spin polarization at the Fermi level [2-4]. They have shown promising advancement in spintronic applications, offering strong spin transport properties and enabling efficient spin currents manipulation. The greater part of predicted half-metallic ferromagnets (HMFs) [5, 6] are found among Heusler compounds, particularly ternary X2YZ materials that crystallize in the L21 structure [7, 8], where X and Y represent transition metals and Z denotes a main s-p group element. Nevertheless, in some ternary Heusler compounds, disordering effects often compromise their half-metallic nature and impact the magneto-resistance ratio [9, 10]. In response to this challenge, recent research has focused on exploring quaternary Heusler alloys to reduce these limitations. The new alloys can be obtained by replacing one of the X atoms in X2YZ with another atom X′, crystallizing in the LiMgPdSn-type crystal structure [11, 12] withF-43m symmetry [13]. In these compounds, the valence of X' is lower than that of X, and the valence of Y is lower than that of both X and X'.

Over the past few decades, quaternary Heusler alloys have garnered significant attention for their low toxicity and unique properties, including half-metallic ferromagnetism (HMF) and high thermoelectric performance. These characteristics placed them as promising materials for applications in spintronics and thermo-electrics devices. Many scientists have concentrated on confirming the half magnetic characteristics in quaternary Heusler alloys that include magnetic transition-metal elements, such as quaternary Heusler ferromagnets CoFeYGe (Y=Cr and Ti) [14], CoFeScZ (Z=P, As, Sb) [15], CoFeCrZ (Z = Al, Si, Ga and Ge) [16]and VZrReZ (Z= Si, Ge and Sn) [17]. Additionally, Ozdogan et al. theoretically investigated 60 quaternary Heusler alloys, finding that 41 of them exhibited half-metallic properties. In today's spintronic research, there is rising attention in materials with high spin polarization at Fermi energy, promising enhanced magneto-resistance and reduced signal-to-noise ratios in devices. The current trend is to explore new types of half-metallic (HM) compounds, specifically d0 or sp HM compounds, which do not include transition metal elements. Compared with the traditional (HMF) quaternary Heusler materials containing transition metal elements that often exhibit large stray magnetic fields, d0 materials are more practical for real-world applications due to their smaller magnetic moments especially in embedded systems in telecommunication applications. Many d0 quaternary Heusler compounds have been predicted, including those studied by Bouabça et al [19] who examined the structural, electronic, magnetic,

Cite as: K. Bahnes, S. Rezini, A. Abbad, W. Benstaali, N. Saidi, O. Belarbi, East Eur. J. Phys. 3, 365 (2025), https://doi.org/10.26565/2312-4334-2025-3-37

and thermal properties of the new quaternary Heusler alloys CsSrCZ (with Z = Si, Ge, Sn, P, As, and Sb), Du et al [20, 21] investigated the electronic structures and magnetic properties of quaternary alloys KCaCZ (Z=F and Cl) and KCaNZ (Z = O, S, and Se) where, all the compounds were found to be HM ferromagnetic materials. Rezaei et al [22] studied RbCaNZ (Z = O, S, and Se) quaternary Heusler compounds. These materials exhibit many interesting features, such as a rather large HM gap and a high Curie temperature, and are robust to the change of the lattice parameter. Moreover, d0 Heusler materials have excellent thermoelectric (TE) properties [23, 24], since they convert efficiently waste heat into electricity, offering benefits such as cost-effectiveness, abundance in nature, and environmental friendliness by avoiding toxic elements.

Nevertheless, to the best of our knowledge, up to now, there is no work on RbCaYF (Y= C and N) compounds on the basis of quaternary Heusler structure that has been done and reported. This is why, in this article, quaternary Heusler compounds RbCaYF (Y= C and N) were predicted by means of density functional calculations. We investigated the structural, electronic, magnetic and thermoelectric properties of the two Heusler alloys to verify the possibility of their application in the fabrication of embedded systems for telecommunication engineering. The organization of this work is as follows: Section 1 provides an overview of previous studies on d0 quaternary Heusler alloys. Section 2 offers a brief description of the crystal structure and computational methods used. Section 3 presents the results and their interpretations. Finally, Section 4 summarizes the key findings of the study.

2. COMPUTATIONAL DETAILS

The full potential linearized augmented plane-wave (FP-LAPW) [25, 26] method of density functional theory (DFT), as implemented in WIEN2k code [27] was employed to study the different properties of the new quaternary Heusler alloys RbCaYF (Y = C and N). The exchange and correlation potential were treated using generalized gradient approximation within the parameterization of Perdew–Burke– Ernzerhof (GGA-PBE) [28, 29] and generalized gradient approximation plus Modified Becke and Johnson (GGA-mBJ) [30, 31]. The muffin-tin sphere radii (RMT) were chosen equal to 2 (a.u) for Rb, Ca, Y = (C and N), and F. The plane wave cut-off (K max) was chosen as 8.0/RMT for the expansion of the wave functions in the interstitial region. The choice of this value is due to the fact that it is usually sufficient to converge the total energy to few meV. The Fourier-expanded charge density was truncated at Gmax=12 $(a.u)^{-1}$ to allow a correct convergence of charge density and to keep a reasonable time of calculation. To achieve self-consistency, a k -points in the irreducible wedge of the Brillouin zone generated from a 14 × 14 × 14 mesh which permit to well describe electronic properties. The cut-off energy was limited by -6 Ry value, which defines the separation of valence and core states, this value is the threshold energy below which states are considered core (deep core) and do not participate in chemical bonds. The energy convergence criterion was set to 10^{-6} Ry per formula unit and the criterion for charge convergence was 10^{-4} electrons during self-consistency cycles. These values are used to stop iterations since the system is considered as convergent with great precision.

The thermoelectric properties are calculated with the BoltzTrap code [32], using 120000 k points.

3. RESULTS AND DISCUSSIONS

3.1. Structural properties

The quaternary Heusler compounds are adopted in LiMgPdSn-type crystal structure designated as Y (space group 216). There are three possible different types of atom arrangement in the quaternary Heusler compound XX'YZ: Y-type(I): X (0, 0, 0), X' (0.25, 0.25, 0.25), Y (0.5, 0.5, 0.5), and Z (0.75, 0.75, 0.75); Y-type(II): X (0.25, 0.25, 0.25), X' (0, 0, 0), Y (0.5, 0.5, 0.5), and Z (0.75, 0.75,0.75); Y-type(III): X (0.25, 0.25, 0.25), X' (0.75, 0.75, 0.75), Y (0, 0, 0), and Z (0.5, 0.5, 0.5). The crystal structures are shown in Fig. 01.

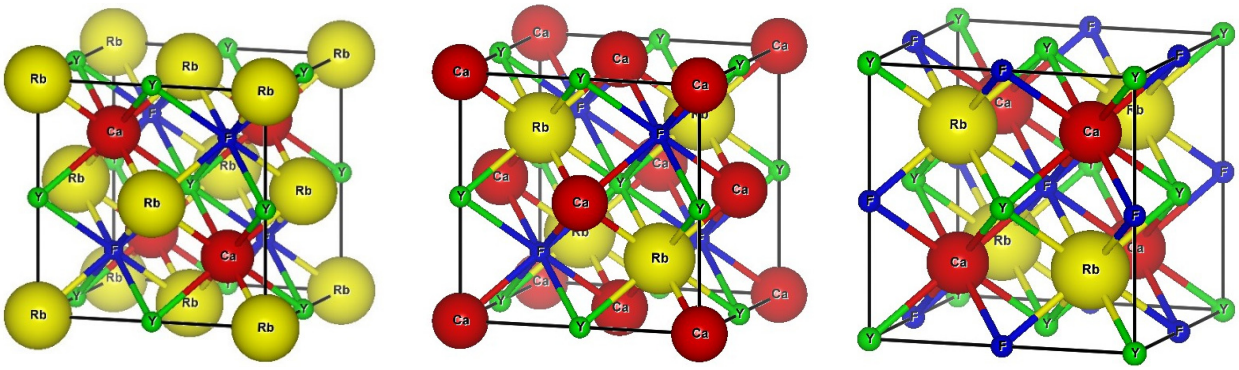

(a) (b) (c)

Figure 1. Visualization of unit cell structure of the RbCaYF (Y = C and N) compounds for (a) Y-type(I) (b) Y-type(II) and (c) Y-type(III) structures using VESTA package

In other to verify the structural and magnetic ground states of the three configurations, the total energies of the non-magnetic (NM) and ferromagnetic (FM) states as a function of the volume were calculated and fitted to the Birch-

Murnaghan's equation of state [33]. The obtained curves are shown in Figures 2 and 3. The results show that Y-type (III) phase is the most favorable structure for both RbCaCF and RbCaNF due to the lowest total energies of equilibrium states. Additionally, the two compounds have the lowest energy in the ferromagnetic state (FM), which indicates that RbCaCF and RbCaNF compounds are most stable in the ferromagnetic state (FM) with the LiMgPdSn-type (III). The energy differences make obvious the significant FM coupling under normal conditions.

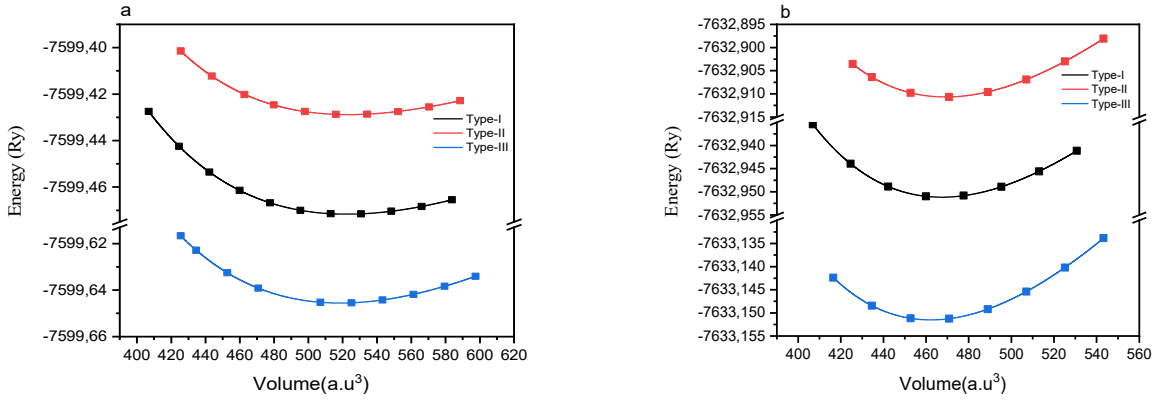

Figure 2. Total energy as a function of unit cell volume for the RbCaCF (a) and RbCaNF (b) compounds in the type-I, type-II, and type-III structures

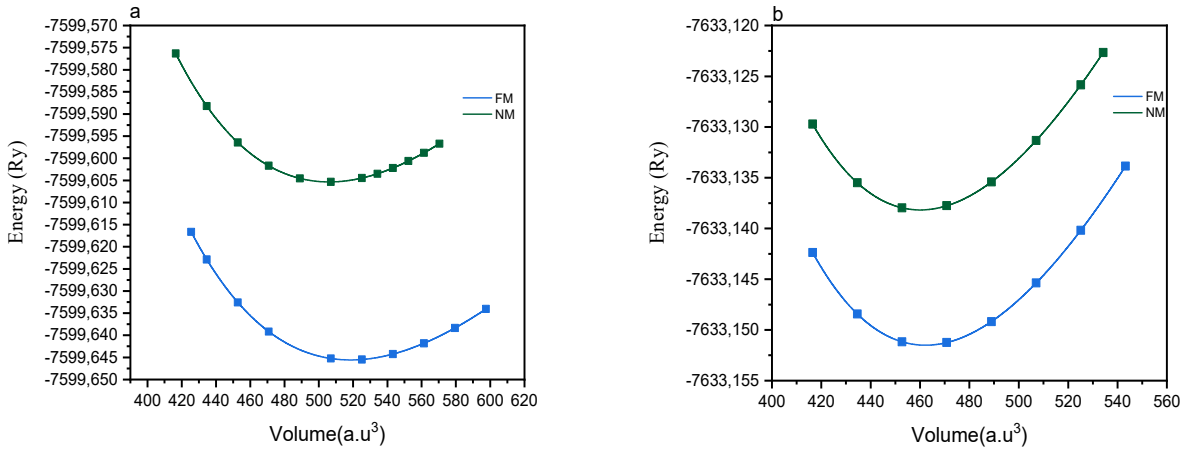

Figure 3. Total energy as a function of unit cell volume in the type-III structures for non-ferromagnetic and ferromagnetic structure for the RbCaCF (a) and RbCaNF (b) compounds

In Table 1, we report our calculated equilibrium lattice constant *a*0, along with bulk modulus B, derivative of bulk modulus B' and the total energies Etot in their different structural and magnetic configurations. As we can see, the obtained equilibrium lattice constant increases with the increase of the atomic radius of anion: 6.49 and 6.74 Å, for RbCaNF and RbCaCF respectively. Moreover, the highest calculated bulk moduli for RbCaYF (Y = C and N) compounds in FM- Y-type (III) configuration confirm the stability of this structure.

Table 1. The calculated bulk parameters, including lattice parameter a_0 (Å), bulk modulus B (GPa), derivative of bulk modulus B', and the total energies Etot (in Ry) per formula unit, of RbCaYF (Y = C and N) compounds in Y-type(I), Y-type(II) and Y-type(III) structures

Alloy	**Structure**	***Phase***	***a0*(Å)**	***B*(GPa)**	**B'**	**E_{tot}(Ry)**
RbCaCF	**Y-type(I)**	**FM**	6.76	31.36	4.78	-7599.471666
	Y-type(II)	**FM**	6.67	28.06	5.49	-7599.428816
	Y-type(III)	**FM**	6.74	36.09	4.27	-7599.645574
		NM	6.69	38.32	4.23	-7599.605348
RbCaNF	**Y-type(I)**	**FM**	6.51	44.53	5.10	-7632.951160
	Y-type(II)	**FM**	6.52	42.43	4.97	-7632.910680
	Y-type(III)	**FM**	6.49	49.14	4.52	-7633.151506
		NM	6.48	50.20	4.47	-7633.138173

3.2. Electronic properties

Using GGA and GGA-mBJ approximations, the spin-polarized electronic band structures of RbCaCF and RbCaNF for both spin-up and spin-down with equilibrium lattice parameters considered in the high symmetry directions of the first Brillouin zone are calculated and shown in Fig. 4 and 5, the Fermi level is set to 0 eV. We can see clearly, that the

spin-up electronic bands exhibit a semiconducting behavior with an indirect band gap where the top of the valence bands is at X point and the bottom of conduction bands is at Γ point. The spin down energy bands have an overlap with the Fermi level and show a metallic characteristic. The two approaches give a similar band structure form with a difference in the gap value. The results obtained, illustrate that the two Heusler alloys are d0 half-metallic ferromagnetic materials with 100% spin polarization and the spin-specific carriers should be sufficiently mobile.

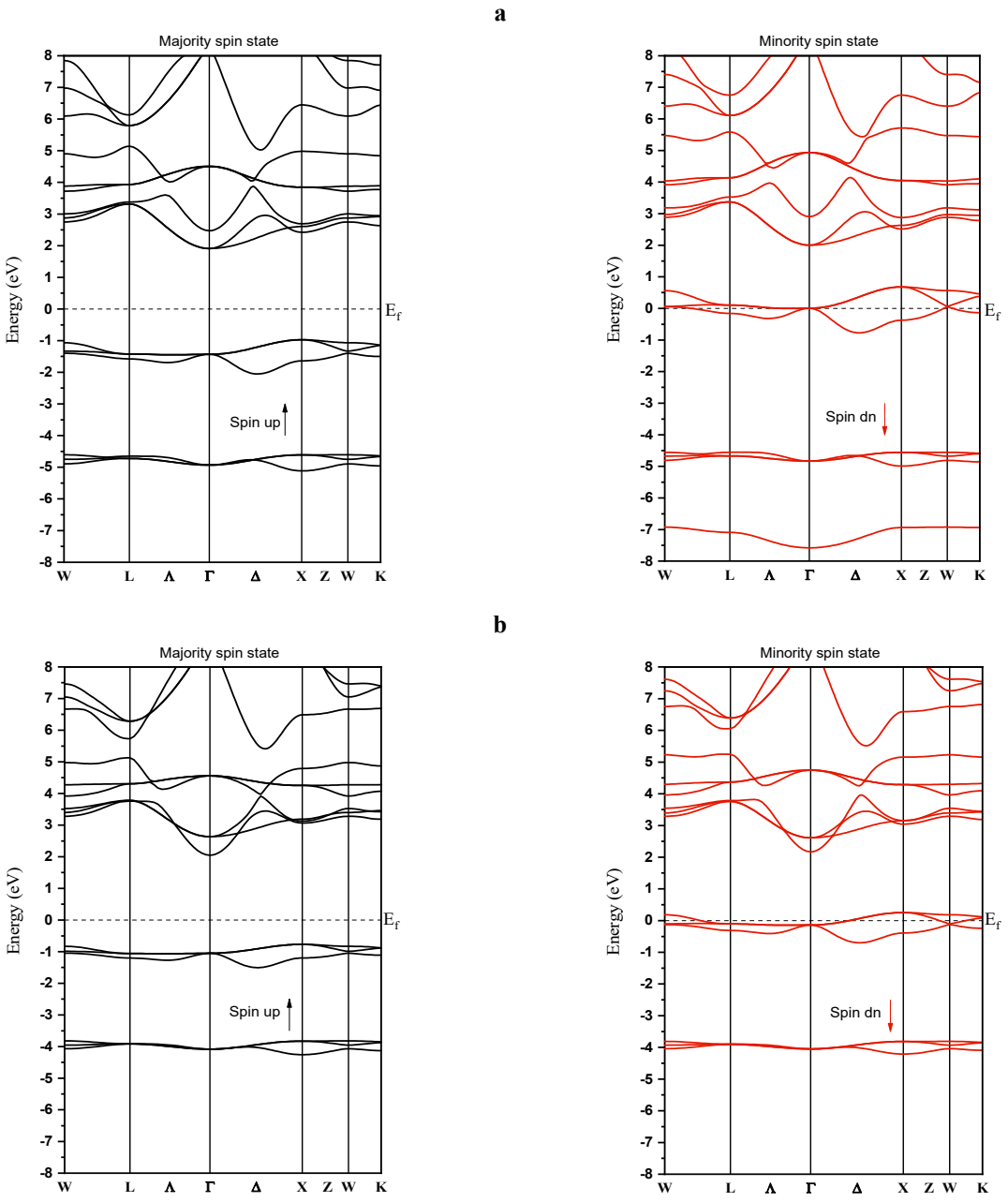

Figure 4. The spin-polarized band structures at the equilibrium lattice parameter of RbCaCF(a) and RbCaNF (b)by using PBE-GGA. Black and red solid lines represent spin-up and spin-down channels, respectively. The dashed line at zero eV indicates the Fermi energy (E_F)

The predicted half-metallic gaps E_{HM} are listed in Table 2. This gap is known to be essential to describe the stability of magnetism of a half-metal [34]. RbCaCF and RbCaNF display large half metallic gaps of 0.879, 0.672 eV using GGA, and 1.730, 1.934 eV with GGA-mBJ respectively illustrating stable half metallic features. Unfortunately, no experimental or theoretical data for the investigated compounds are available for eventual comparison. The calculated density of states (DOS) and partial density of states (PDOS) of RbCaCF and RbCaNF using GGA and GGA-mBJ approximations are shown in Fig. 6 and 7. In order to understand the contribution of each orbital in these atoms we have plotted the angular momentum decomposition of partial density of states. The two compounds have a similar structure. The DOS confirm that majority spin states show semiconducting nature and minority spin states are metallic demonstrating 100% spin polarization at the Fermi level, which is in a good agreement with the band structure calculations. For RbCaCF, and using

GGA the lowest structure extended from -5 eV to -4.5 eV originates mainly from F-p states. The second region from -2eV to 1eV is due to C-p states with a little contribution of Ca-d states.

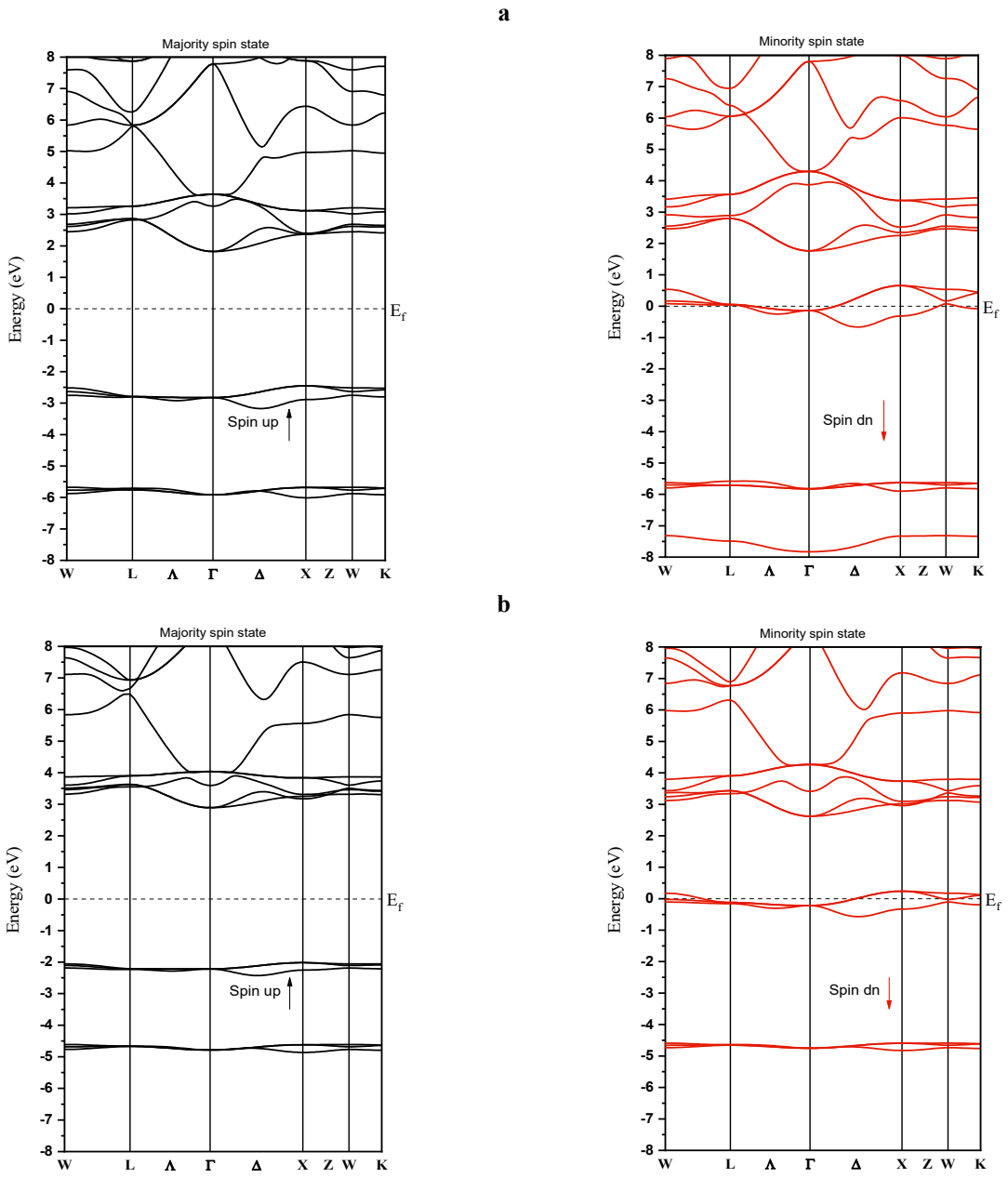

Figure 5. The spin-polarized band structures at the equilibrium lattice parameter of RbCaCF(a) and RbCaNF(b) by using PBE-GGA-mBJ. Black and red solid lines represent spin-up and spin-down channels, respectively. The dashed line at zero eV indicates the Fermi energy (E_F)

Table 2. The virtual semiconducting gap *Eg* (eV), the half-metallic gap E_{HM} (eV) in quaternary Heusler compounds RbCaYF (Y= C and N)

Alloy	Approximations	VBM	CBM	E_g	E_{HM}
RbCaCF	**GGA**	-0.879	1.814	2.693	0.879
RbCaCF	**GGA-Mbj**	-2.351	1.730	4.081	1.730
RbCaNF	**GGA**	-0.672	1.966	2.639	0.672
RbCaNF	**GGA-Mbj**	-1.934	2.800	4.734	1.934

Hence, the spin polarization is mainly attributed to the contribution of p-d hybridization between C and Ca atoms. The structure from the conduction band minima and above presents a large contribution from Ca-d states. For RbCaNF, the same trend is observed. To realize more realistic electronic density of states, and to overcome the well-known deficiency of DFT regarding energy gap underestimation with GGA functional, and to obtain the exact energy gaps, we

employ the GGA-mBJ as exchange correlation potential and recalculate the spin polarization band structures. The bandgap values computed according to GGA–PBE and GGA–mBJ are listed in Table 02. The major difference observed between GGA–PBE and GGA–mBJ calculations is that the GGA–PBE has underestimated the band gap. By using GGA-mBJ functional corrections, we can see clearly that F-p and C-p states in spin up channels, are shifted downwards Valence Band Maximum (VBM) (from -0.879 eV with GGA to -2.351 eV with GGA–mBJ for RbCaCF and from -0.672 eV with GGA to -1.934 eV with GGA–mBJ for RbCaNF) since GGA–mBJ produces better band splitting. The conduction band still predominantly composed from Rb-d and Ca-d states.

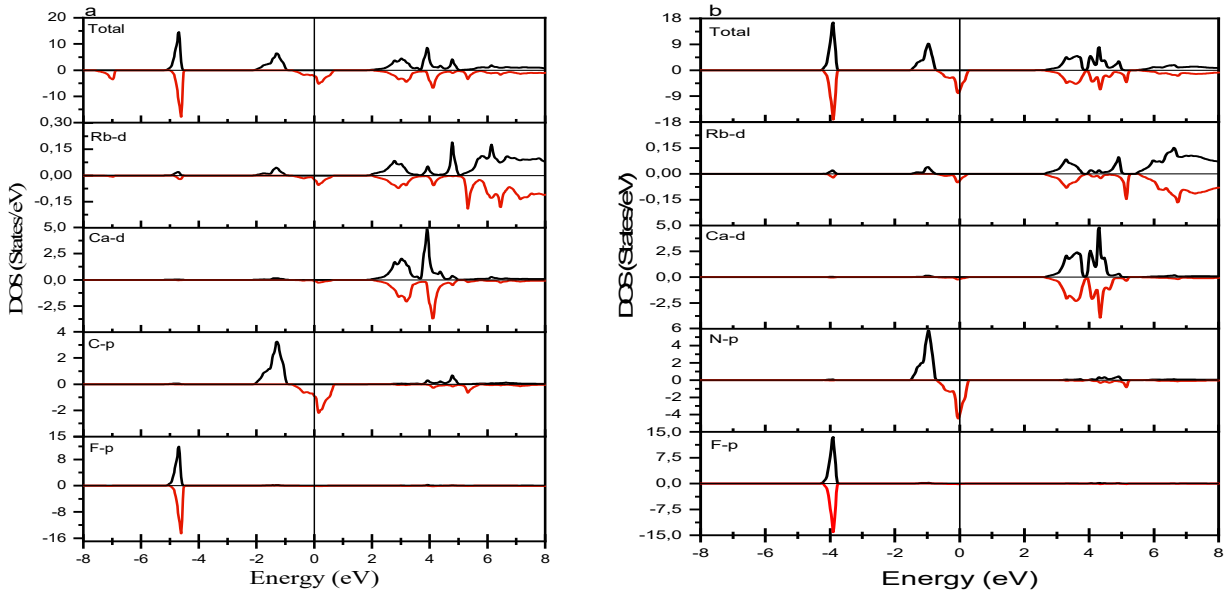

Figure 6. The total and orbital spin-density of states (DOSs) of ferromagnetic forRbCaCF (a) and RbCaNF (b) compounds by using PBE-GGA. Black and red solid lines represent spin-up and spin-down channels, respectively

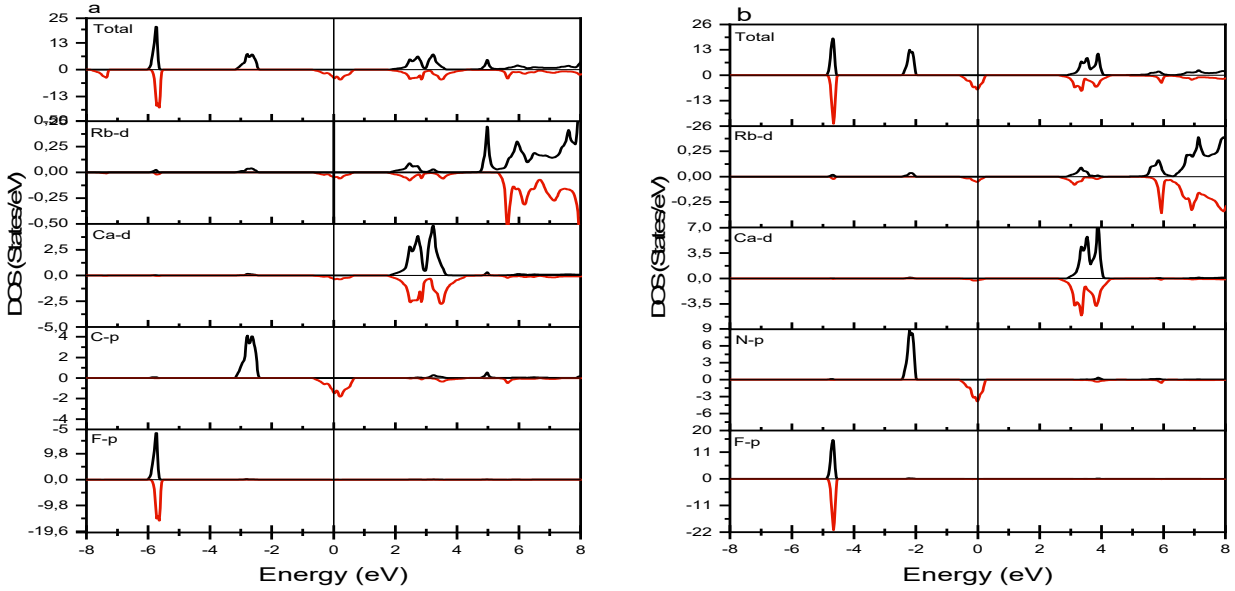

Figure 7. The total and orbital spin-density of states (DOSs) of ferromagnetic for RbCaCF (a) and RbCaNF (b) compounds by using PBE-GGA-mBJ. Black and red solid lines represent spin-up and spin-down channels, respectively

3.3. Magnetic properties

The calculated magnetic moments of Rb, Ca, Y = (C and N), and F along with total and interstitial magnetic moments are reported in table 3. So, the total magnetic moments μ_{tot} of RbCaCF and RbCaNF compounds are integer with $2\mu_B$ and $1\mu_B$ values respectively. The integer total magnetic moment is a characteristic of (HMFs). We can easily explain these values from the electronic configurations of the two compounds. There are 14 (15) valence electrons in RbCaCF and RbCaNF respectively: (Rb: $5s^1$, Ca: $4s^2$, N: $2s^2$, 2p3, F: $2s^2$, $2p^5$ and C: $2s^2$, $2p^2$) which contribute to the magnetism and bond formation. So, 4 valence electrons occupy the F-2s states in the lowest energy states. 6 of the remaining 10 (11) valence electrons occupy the majority spin p states, which results in the 6 fully filled majority spin bands. The remaining 4 (5) valence electrons partially occupy the 6 lowest minority spin bands. The 2 (1) holes remaining are responsible for

the magnetic moments of $2\mu_B$ and $1\mu_B$, respectively. In addition, the total magnetic moment of RbCaYF (Y = C and N) contains five contributions: Rb atom, Ca atom, F atom, Y atom and the interstitial region. We can see clearly from Table 3, that the magnetic moments of the two compounds originate mainly from the p electrons of C and N atoms. The magnetic moment of the Y atom is parallel to that of Rb atom which confirms the ferromagnetism of the 2 full Heuslers. Since the total magnetic moments are integer, they verify the Slater-Pauling rule which is described by the following formula: $\mu_{Tot} = 12\text{-}Nv$; where μ_{Tot} means the total spin magnetic moment and Nv is the total number of valence electrons per unit-cell. The RbCaYF (Y = C and N) compounds have 10 and 11 valence electrons respectively, so the calculated μ_{tot} for the two compounds satisfy the formula cited above.

Table 3. The calculated atomic magnetic moments M (μ_B) for the RbCaYF(Y=C and N) alloys

Alloy	M_{tot}	M_{Rb}	M_{Ca}	M_Y	M_F	M_{int}
RbCaCF	2.00	0.048	0.047	1.169	0.039	0.699
RbCaNF	1.00	0.016	-0.004	0.794	0.009	0.184

3.4. Thermoelectric properties

Continuing research focuses on finding new Heusler structures and compositions with enhanced thermoelectric performance, by exploring different combinations of X, Y, and Z elements, in addition to examining the effects of several synthesis and processing techniques. Thermoelectric Efficiency is classically measured by the dimensionless figure of merit ZT, which is given by the formula: $ZT=S^2\sigma T/k$ where S is the Seebeck coefficient (thermo-power), σ is the electrical conductivity, T is the absolute temperature, and k is the thermal conductivity. Heusler alloys can exhibit high Seebeck coefficients depending on their composition and the temperature range. A high Seebeck coefficient is attractive for efficient thermoelectric materials as it indicates a large voltage for a given temperature difference. Since quaternary Heusler materials are regarded as the alternate sources of energy because of their aptitude to convert waste heat into electricity and are used for power generation as they are abundant in nature, and principally environmentally friendly, we report in this study and for the first time, Seebeck coefficient: S, electrical conductivity: σ/τ, thermal conductivity: k/τ and figure of merit ZT of the new d0 quaternary Heusler compounds RbCaYF (Y= C and N) using BoltzTrap code. The different parameters are presented on Figures 8 (a), (b), (c) and (d).

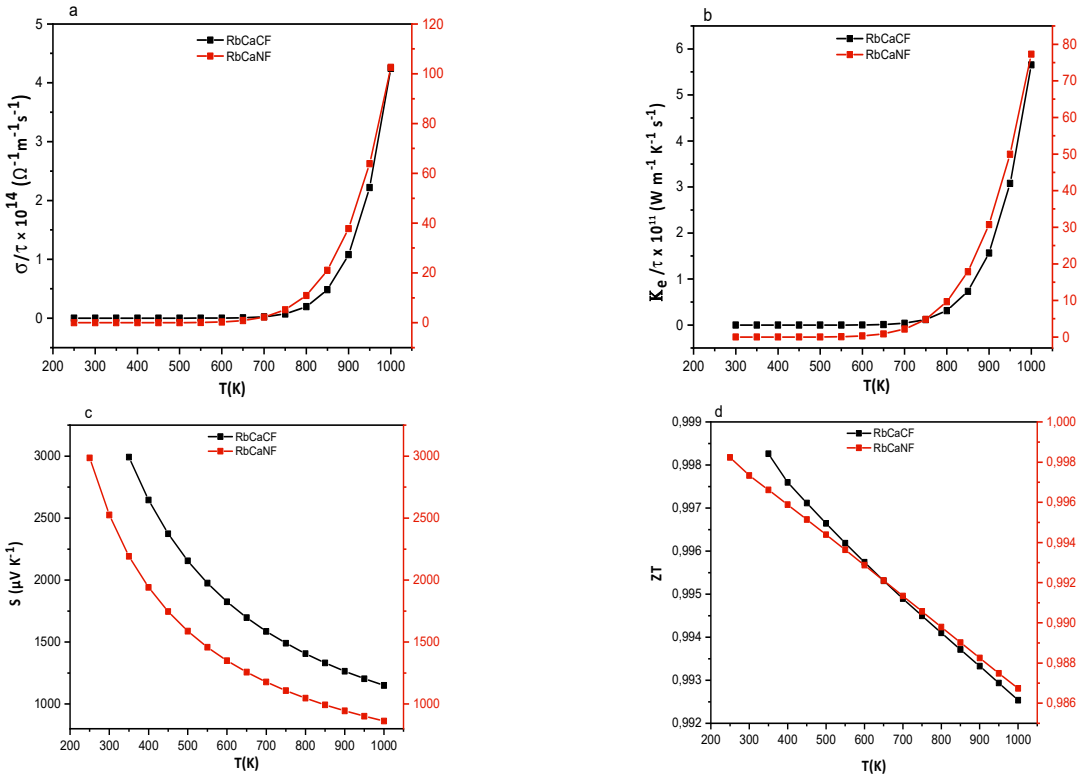

Figure 8. The variation of total electrical conductivity σ/τ (a), total thermal conductivity k/τ (b), total Seebeck coefficient S (c) and figure of merit ZT (d) as a function of temperature for RbCaYF (Y= C and N) compounds

The temperature variation of electrical conductivity σ/τ is reported in Fig. 8 (a). We observe that the electrical conductivity of the two compounds is nearly zero at room temperature but increases exponentially with increasing temperature, at 1000 K it attains 4.24×10^{14} /Ωms and 102.56×10^{14} /Ωms for RbCaCF and RbCaNF, respectively, so RbCaNF shows high electric conductivity comparing to RbCaNF which is consistent with the band structure investigations. In Fig. 8(b), we present the variation of total thermal conductivity k/τ with temperature. It is obvious

that k/τ plots follow a similar trend as those of electrical conductivity σ/τ. The k/τ values show a negligible variation up to 750 k and increases at higher temperatures. It reaches 5.65×10^{10} /WK^{2}ms and 77.31×10^{10} /WK^{2}ms for RbCaCF and RbCaNF, respectively. Figure 8 (c) displays the variation of Seebeck coefficient with the temperature. As we can see, the Seebeck coefficient RbCaYF (Y= C and N) of the two Heusler compounds is positive for the entire temperature range which explains that the holes are dominant charge carriers, therefore RbCaYF are *p*-type materials essential in thermoelectric applications, such as power generation from waste heat and energy-efficient cooling devices. S decreases exponentially with increasing temperature. The values of Seebeck coefficient are 1150 μV/K and 862 μV/K for RbCaCF and RbCaNF at 1000 K respectively. Finally, we calculated the figure of merit ZT which is an essential parameter for assessing the efficiency of thermoelectric materials and devices. High ZT value indicates a more efficient thermoelectric material. A figure of merit ZT equal to 1 signifies that a thermoelectric material has achieved equilibrium between electrical conductivity, Seebeck coefficient, and thermal conductivity [35]. The variation of ZT with temperature for the two Heuslers alloys, is shown on Fig. 8(d), ZT decreases slightly in the large temperature range 200-1000 K, it stills close to the unity for the two compounds. These results suggest the excellent thermoelectric performance of these two d0 Heuslers alloys signifying that they could be promising materials for applications in thermoelectric technologies in particular at high temperatures for example in industrial processes or power plants, so these materials can convert excess heat into electrical power which improves efficiency with reducing energy waste or in space Exploration, they can be very benefit, where they power spacecrafts and rovers.

4. CONCLUSION

To summarize, the structural, electronic magnetic and thermoelectric properties of new d0 quaternary Heuslers compounds RbCaYF (Y = C and N) are predicted using full-potential linearized augmented plane wave (FP-LAPW) method of density functional theory (DFT) within the generalized gradient approximation (GGA) and generalized gradient approximation plus Modified Becke and Johnson (GGA-mBJ). The stable type Y-type (III) configuration structure in the ferromagnetic state (FM) was energetically more favorable due to the lowest total energies of equilibrium states. The two systems are predicted to be HM ferromagnets with a large half metallic gap of 0.879, 0.672 eV using GGA, and 1.730, 1.934 eV with mBJ for RbCaCF and RbCaNF respectively. The use of the modified Becke–Johnson exchange potential approximation (GGA-mBJ) improves the results found by the standard-GGA since it gives an apparent picture of the electronic structure at the Fermi level. The total magnetic moments μ_{tot} of RbCaCF and RbCaNF compounds are integer with $2\mu_B$ and $1\mu_B$ values respectively. The origin of ferromagnetism is the polarization of the p-orbitals of N and C atoms with an sp-hybridization. Additionally, the transport properties of the two compounds predict that the two compounds may perform well particularly at high temperatures. These materials exhibit high values of electric conductivity and figure of merit at 1000K where their application becomes particularly interesting nevertheless, further investigations are required to minimize thermal conductivity and enhance Seebeck coefficient at high temperatures. RbCaCF and RbCaNF d0 Heusler alloys present high spin polarization, robust half-metallicity and high thermoelectric coefficients which makes them good candidates for spintronic and thermoelectric applications. In addition, our Heusler alloys have significant potential for enhancing embedded systems used in telecommunications through their use in spintronics, magnetic sensors, magnetoresistive devices and high-frequency applications. A good number of the investigated properties are reported for the first time and are opened for experimental verification.

Declaration of Funding: No funding was received for this study.

ORCID

Kheira Bahnes, https://orcid.org/0009-0007-3676-1126; **Wissam Benstaali,** https://orcid.org/0000-0003-4634-6210
Noureddine Saidi, https://orcid.org/0009-0004-5343-8572; **Omar Belarbi,** https://orcid.org/0009-0002-6504-359X
Amel Abbad, https://orcid.org/0009-0006-1622-5564; **Saliha Rezini,** https://orcid.org/0000-0002-8080-3051

REFERENCES

[1] R.A. De Groot, F.M. Mueller, P.V. van Engen, and K.H.J. Buschow, (1983). "New class of materials: half-metallic ferromagnets," Physical review letters, **50**(25), 2024-2027 (2024). https://doi.org/10.1103/PhysRevLett.50.2024
[2] P.J. Brown, K.U. Neumann, P.J. Webster, and K.R.A. Ziebeck, "The magnetization distributions in some Heusler alloys proposed as half-metallic ferromagnets," J. Phys.Condens. Matter, **12**, 1827 (2000). https://doi.org/10.1088/0953-8984/12/8/325
[3] T. Graf, C. Felser, and S.S. Parkin, "Simple rules for the understanging of Heusler compounds," Prog. Solid State Ch. **39**, 1-50 (2011). https://doi.org/10.1016/j.progsolidstchem.2011.02.001
[4] C. Felser, I. Wollmann, S. Chadov, G.H. Fecher, and S.S. Parkin, "Basics and perspective of magnetic Heusler compounds," APL Mater. **3**, 041518 (2015). https://doi.org/10.1063/1.4917387
[5] J.M.D. Coey, M. Venkatesan, and M.A. Bari, "Half-Metallic Ferromagnets," in: *High Magnetic Fields. Lecture Notes in Physics*, vol. 595, edited by C. Berthier, L.P. Lévy, and G. Martinez, (Springer-Verlag, NY, 2002), pp. 377–396. https://doi.org/10.1007/3-540-45649-X_15
[6] I. Zutic, J. Fabian, and S.D. Sharma, "Spintronics: Fundamentals and applications," Rev. Mod. Phys. **76**, 323 (2004). https://doi.org/10.1103/RevModPhys.76.323
[7] Galanakis, Ph. Mavropoulos, and P.H. Dederichs, "Electronic structure and Slater–Pauling behaviour in half-metallic Heusler alloys calculated from first principles," J. Phys. D: Appl. Phys. **39**, 765 (2006). https://doi.org/10.1088/0022-3727/39/5/S01

[8] H. Kurt, K. Rode, M. Venkatesan, P. Stamenov, and J.M.D. Coey, "High spin polarization in epitaxial films of ferrimagnetic Mn_3Ga," Phys. Rev. B, **83**, 020405(R) (2011). https://doi.org/10.1103/PhysRevB.83.020405; "$Mn_{3-x}Ga$ $(0 \leq x \leq 1)$: Multifunctional thin film materials for spintronics and magnetic recording," Phys. Status Solidi B, **248**, 2338 (2011). https://doi.org/10.1002/pssb.201147122
[9] Y. Miura, K. Nagao, and M. Shirai, "Atomic disorder effects on half-metallicity of the full-Heusler alloys $Co_2(Cr_{1-x}Fex)Al$: A first-principles study," Phys. Rev. B, **69**, 144413 (2004). https://doi.org/10.1103/PhysRevB.69.144413
[10] H.C. Kandpal, V. Ksenofontov, M. Wojcik, R. Seshadri, and C. Felser, "Electronic structure, magnetism and disorder in the Heusler compound Co_2TiSn," J. Phys. D: Appl. Phys. **40**, 1587 (2007). https://doi.org/10.1088/0022-3727/40/6/S13
[11] X. Dai, G. Liu, G.H. Fecher, C. Felser, Y. Li, and H. Liu, "New quaternary half metallic material CoFeMnSi," J. Appl. Phys. **105**, 07E901 (2009). https://doi.org/10.1063/1.3062812
[12] G.Z. Xu, E.K. Liu, Y. Du, G.J. Li, G.D. Liu, W.H. Wang, and G.H. Wu, "A new spin gapless semiconductors family: Quaternary Heusler compounds," EPL, **102**, 17007 (2013). https://doi.org/10.1209/0295-5075/102/17007
[13] J. Drews, U. Eberz, and H. Schuster, "Optische Untersuchungen an farbigen Intermetallischen Phasen," J. Less-Common Met. **116**, 271 (1986). https://doi.org/10.1016/0022-5088(86)90235-3
[14] Z. Charifi, T. Ghellab, H. Baaziz, and F. Soyalp, "Characterization of quaternary Heusler alloys CoFeYGe (Y= Ti, Cr) with respect to structural, electronic, magnetic, mechanical, and thermoelectric features," International Journal of Energy Research, **46**(10), 13855-13873 (2022). https://doi.org/10.1002/er.8104
[15] Q. Gao, L. Li, G. Lei, J.B. Deng, and X.R. Hu, "A first-principle study on the properties of a new series of quaternary Heusler alloys CoFeScZ (Z= P, As, Sb)," Journal of Magnetism and Magnetic Materials, **379**, 288-293 (2015). https://doi.org/10.1016/j.jmmm.2014.12.025
[16] M.I. Khan, H. Arshad, M. Rizwan, S.S.A. Gillani, M. Zafar, S. Ahmed, and M. Shakil, "Investigation of structural, electronic, magnetic and mechanical properties of a new series of equiatomic quaternary Heusler alloys CoYCrZ (Z= Si, Ge, Ga, Al): A DFT study," Journal of Alloys and Compounds, **819**, 152964 (2020). https://doi.org/10.1016/j.jallcom.2019.152964
[17] F. Faid, H. Mebarki, K. Mokadem, F.M. Abdalilah, A. Benmakhlouf, M. Khatiri, and T. Helaimia, "Systematic study of structural, elastic, electronic, Magnetism and Half-metallic properties for the quaternary alloys: Heusler type VZrReZ (Z= Si, Ge and Sn)," Journal of Magnetism and Magnetic Materials, 172345 (2024). https://doi.org/10.1016/j.jmmm.2024.172345
[18] K. Özdoğan, E. Şaşıoğlu, and I. Galanakis, "Slater-Pauling behavior in LiMgPdSn-type multifunctional quaternary Heusler materials: Half-metallicity, spin-gapless and magnetic semiconductors," Journal of Applied Physics, **113**(19), 193903 (2013). https://doi.org/10.1063/1.4805063
[19] A. Bouabça, H. Rozale, A. Amar, X.T. Wang, A. Sayade, and A. Chahed, "First-principles study of new series of quaternary Heusler alloys CsSrCZ (Z=Si, Ge, Sn, P, As, and Sb)," J. Magn. Magn. Mater. **419**, 210-217 (2016). https://doi.org/10.1016/j.jmmm.2016.06.018
[20] J. Du, S. Dong, Y.L. Lua, H. Zhao, L.F. Feng, and L.Y. Wang, "Half-metallic ferromagnetic features in d^0 quaternary-Heusler compounds KCaCF and KCaCCl: A first-principles description," J. Magn. Magn. Mater, **428**, 250-254 (2017). https://doi.org/10.1016/j.jmmm.2016.12.038
[21] J. Du, S. Dong, X.T. Wang, H. Rozale, H. Zhao, L.Y. Wang, and L.F. Feng, "Half-metallic ferromagnetism in KCaNX (X = O, S, and Se) quaternary Heusler compounds: A first-principles study," Superlattices Microstruct, **105**, 39-47 (2017). https://doi.org/10.1016/j.spmi.2016.12.055
[22] S. Rezaei, and F. Ahmadian, "First-principles study of half-metallic properties in RbCaNZ (Z = O, S, and Se) quaternary Heusler compounds," J. Magn. Magn. Mater, **456**, 78-86 (2018). https://doi.org/10.1016/j.jmmm.2018.02.006
[23] A. Taleb, A. Chahed, M. Boukli, H. Rozale, B. Amrani, M. Rahmoune, and A. Sayede, "Structural, magneto-electronic and thermophysical properties of the new d0 quaternary heusler compounds KSrCZ (Z= P, As, Sb)," Revista mexicana de física, **66**(3), 265-272 (2020). https://doi.org/10.31349/RevMexFis.66.265
[24] S. Gheriballah, B. Bouabdellah, A. Oughilas, M.A. Boukli, M. Rahmoune, and A. Sayede, "Investigating structure, magneto-electronic, and thermoelectric properties of the new d0 quaternary Heusler compounds RbCaCZ (Z= P, As, Sb) from first principle calculations," Indian Journal of Pure & Applied Physics, **58**, 818-824 (2020). https://doi.org/10.56042/ijpap.v58i11.32390
[25] P. Hohenberg, and W.J.P.R. Kohn, "Inhomogeneous Electron Gas," Phys. Rev. B, **136**, B864-B871 (1964). http://dx.doi.org/10.1103/PhysRev.136.B864
[26] J.P. Perdew, J.A. Chevary, S.H. Vosko, K.A. Jackson, M.R. Pederson, D.J. Singh, and C. Fiolhais, "Atoms, molecules, solids, and surfaces: Applications of the generalized gradient approximation for exchange and correlation," Phys. Rev. B, **46**, 6671 (1992). https://doi.org/10.1103/PhysRevB.46.6671
[27] P. Blaha, K. Schwarz, G. K. Madsen, D. Kvasnicka, J. Luitz, *et al.*, "WIEN2k. An augmented plane wave+ local orbitals program for calculating crystal properties," **60**, 155 (2001).
[28] J.P. Perdew, K. Burke, and M. Ernzerhof, "Generalized gradient approximation made simple," Physical review letters, **77**(18), 3865 (1996). https://doi.org/10.1103/PhysRevLett.77.3865
[29] J.P. Perdew, and Y. Wang, "Accurate and simple analytic representation of the electron-gas correlation energy," Phys. Rev. B, **45**, 13244 (1992). https://doi.org/10.1103/PhysRevB.45.13244
[30] F. Tran, P. Blaha, and K. Schwarz, "Band gap calculations with Becke–Johnson exchange potential," Journal of Physics: Condensed Matter, **19**, 196208 (2007). https://doi.org/10.1088/0953-8984/19/19/196208
[31] D. Koller, F. Tran, and P. Blaha, "Improving the modified Becke-Johnson exchange potential," Physical Review B, **85**(15), 155109 (2012). https://doi.org/10.1103/PhysRevB.85.155109
[32] G.K.H. Madsen, and D.J. Singh, "BoltzTraP.A code for calculating band-structure dependent quantities," Computer Physics Communications, **175**(1), 67-71 (2006). https://doi.org/10.1016/j.cpc.2006.03.007
[33] F.D. Murnaghan, "The Compressibility of Media under Extreme Pressures," Proc. Natl. Acad. Sci. USA, **30**, 244-247 (1944). https://doi.org/10.1073/pnas.30.9.244
[34] E. Şaşioglu, L.M. Sandratskii, and P. Bruno, "First-principles study of exchange interactions and Curie temperatures of half-metallic ferrimagnetic full Heusler alloys Mn2V Z (Z = Al, Ge)," J. Phys.: Condens. Matter, **17**, 995 (2005). https://doi.org/10.1088/0953-8984/17/6/017

[35] T. Takeuchi, “Conditions of Electronic Structure to Obtain Large Dimensionless Figure of Merit for Developing Practical Thermoelectric Materials,” Mater. Trans. **50**, 2359-2365 (2009). https://doi.org/10.2320/matertrans.M2009143

МАГНІТНІ ТА ТЕРМОЕЛЕКТРИЧНІ ВЛАСТИВОСТІ СПЛАВІВ ГЕЙСЛЕРА RbCaYF(Y = C та N): ПЕРСПЕКТИВНІ КАНДИДАТИ ДЛЯ ВБУДОВАНИХ СИСТЕМ У ТЕЛЕКОМУНІКАЦІЯХ

Хейра Банес[a,b], Саліха Резіні[b], Амель Аббад[a,b], Віссам Бенстаалі[a,b], Нуреддін Саїді[a,b], Омар Беларбі[a,b]

[a]*Лабораторія технологій та властивостей твердих тіл, Факультет наук і технологій, Університет Абдельхаміда Ібн Бадіса, Мостаганем, Алжир*

[b]*Факультет наук і технологій, BP227, Університет Абдельхаміда Ібн Бадіса, Мостаганем (27000), Алжир*

На основі теорії функціоналу густини було проаналізовано структурні, електронні, магнітні та термоелектричні властивості нових четвертинних сплавів Гейслера d0 RbCaYF (Y = C та N) за допомогою розрахунків з перших принципів. Результати передбачають стабільне розташування атомів у фазі Y-типу (III) з феромагнітним порядком. Було виявлено, що дві сполуки є напівметалевими феромагнетиками (HMF) з цілочисельним магнітним моментом 2 μ_B для RbCaCF та 1 μ_B для RbCaNF. Спостережуваний феромагнетизм походить від поляризації p-Y орбіталей з sp2-гібридизацією. Крім того, RbCaCF та RbCaNF демонструють великі напівметалеві (HM) щілини 0,879, 0,672 еВ за допомогою узагальненого градієнтного наближення (GGA) та 1,730, 1,934 еВ відповідно за допомогою узагальненого градієнтного наближення модифікованого методу Бекке-Джонсона (GGA-mBJ), демонструючи стабільні напівметалеві характеристики. Крім того, термоелектричні властивості були розраховані в широкому діапазоні температур. Два сплави Гейслера демонструють високі значення електропровідності та коефіцієнта якості, особливо за високих температур. Сплави Гейслера RbCaCF та RbCaNF d0 мають високу спінову поляризацію, стійку напівметалевість та високі термоелектричні коефіцієнти, що робить їх хорошими кандидатами для спінтроніки та термоелектричних застосувань, що призводить до багатообіцяючих удосконалень вбудованих систем у телекомунікаціях.

Ключові слова: *напівметал; d0 сплави Гейслера; вбудовані системи; термоелектричні властивості; телекомунікації; Wien2k*